

SCIENTIFIC REPORTS



OPEN

Disassembly of the self-assembled, double-ring structure of proteasome $\alpha 7$ homo-tetradecamer by $\alpha 6$

Received: 01 October 2015
Accepted: 13 November 2015
Published: 14 December 2015

Kentaro Ishii¹, Masanori Noda², Hirokazu Yagi³, Ratsupa Thammaphorn^{4,5}, Supaporn Seetaha^{4,5}, Tadashi Satoh^{3,6}, Koichi Kato^{1,3,5} & Susumu Uchiyama^{1,2}

The 20S core particle of the eukaryotic proteasome is composed of two α - and two β -rings, each of which is a hetero-heptamer composed of seven homologous but distinct subunits. Although formation of the eukaryotic proteasome is a highly ordered process assisted by assembly chaperones, $\alpha 7$, an α -ring component, has the unique property of self-assembling into a homo-tetradecamer. We used biophysical methods to characterize the oligomeric states of this proteasome subunit and its interaction with $\alpha 6$, which makes direct contacts with $\alpha 7$ in the proteasome α -ring. We determined a crystal structure of the $\alpha 7$ tetradecamer, which has a double-ring structure. Sedimentation velocity analytical ultracentrifugation and mass spectrometric analysis under non-denaturing conditions revealed that $\alpha 7$ exclusively exists as homo-tetradecamer in solution and that its double-ring structure is disassembled upon the addition of $\alpha 6$, resulting in a 1:7 hetero-octameric $\alpha 6$ - $\alpha 7$ complex. Our findings suggest that proteasome formation involves the disassembly of non-native oligomers, which are assembly intermediates.

The proteasome, a huge protein complex responsible for ubiquitin-dependent proteolysis in eukaryotic cells^{1,2}, is composed of a 20S core particle, which serves as a proteolytic chamber, and one or two regulatory particles³. The core particle consists of two α - and two β -rings, which form a cylindrical, four-layered $\alpha\beta\beta\alpha$ structure^{4,5}. The α -ring is composed of seven homologous but distinct subunits, $\alpha 1$ – 7 , that are arranged into a hetero-heptameric structure in the order $\alpha 1$ - $\alpha 2$ - $\alpha 3$ - $\alpha 4$ - $\alpha 5$ - $\alpha 6$ - $\alpha 7$ with assistance of assembly chaperones^{6,7}. Subsequently, seven homologous and distinct β subunits, i.e., $\beta 1$ – 7 , are recruited to specific positions on the α -ring⁸.

Among human proteasome α subunits, $\alpha 7$ exhibits a unique feature of *in vitro* self-assembly into a homo-tetradecamer with a double ring structure^{9,10}. This raises the question whether the $\alpha 7$ homo-tetradecamer is an off-pathway, dead-end product during proteasome formation. Another possibility is that certain mechanisms exist for disassembling the homo-oligomer of the $\alpha 7$ subunit, resulting in its monomeric form, which is a component of the hetero-heptameric α -ring. To resolve this issue, a conventional experimental method is required for characterizing the oligomeric states of proteasome subunits.

Mass spectrometry (MS) under non-denaturing conditions and sedimentation velocity analytical ultracentrifugation (SV-AUC) offer a powerful combination for analyzing biomacromolecular complexes¹¹. The MS method enables us to determine the stoichiometry of the complex by observing accurate biomolecular masses. However, it is rather difficult to obtain quantitative information, for example, regarding the amounts of the molecules in the complexed and free states in solution. In contrast, SV-AUC enables us to determine the quantitative distribution of free and oligomeric species existing in solution, although the accuracy of mass determination in this method

¹Okazaki Institute for Integrative Bioscience, National Institutes of Natural Sciences, 5-1 Higashiyama, Myodaiji, Okazaki, Aichi 444-8787, Japan. ²Department of Biotechnology, Graduate School of Engineering, Osaka University, 2-1 Yamadaoka, Suita, Osaka 565-0871, Japan. ³Graduate School of Pharmaceutical Sciences, Nagoya City University, 3-1 Tanabe-dori, Mizuho-ku, Nagoya, Aichi 467-8603, Japan. ⁴Faculty of Science, Kasetsart University, Bangkok, Bangkok 10900, Thailand. ⁵Institute for Molecular Science, National Institutes of Natural Sciences, 5-1 Higashiyama, Myodaiji, Okazaki, Aichi 444-8787, Japan. ⁶JST, PRESTO, 3-1 Tanabe-dori, Mizuho-ku, Nagoya, Aichi 467-8603, Japan. Correspondence and requests for materials should be addressed to K.K. (email: kkatonmr@ims.ac.jp) or S.U. (email: suchu@bio.eng.osaka-u.ac.jp)

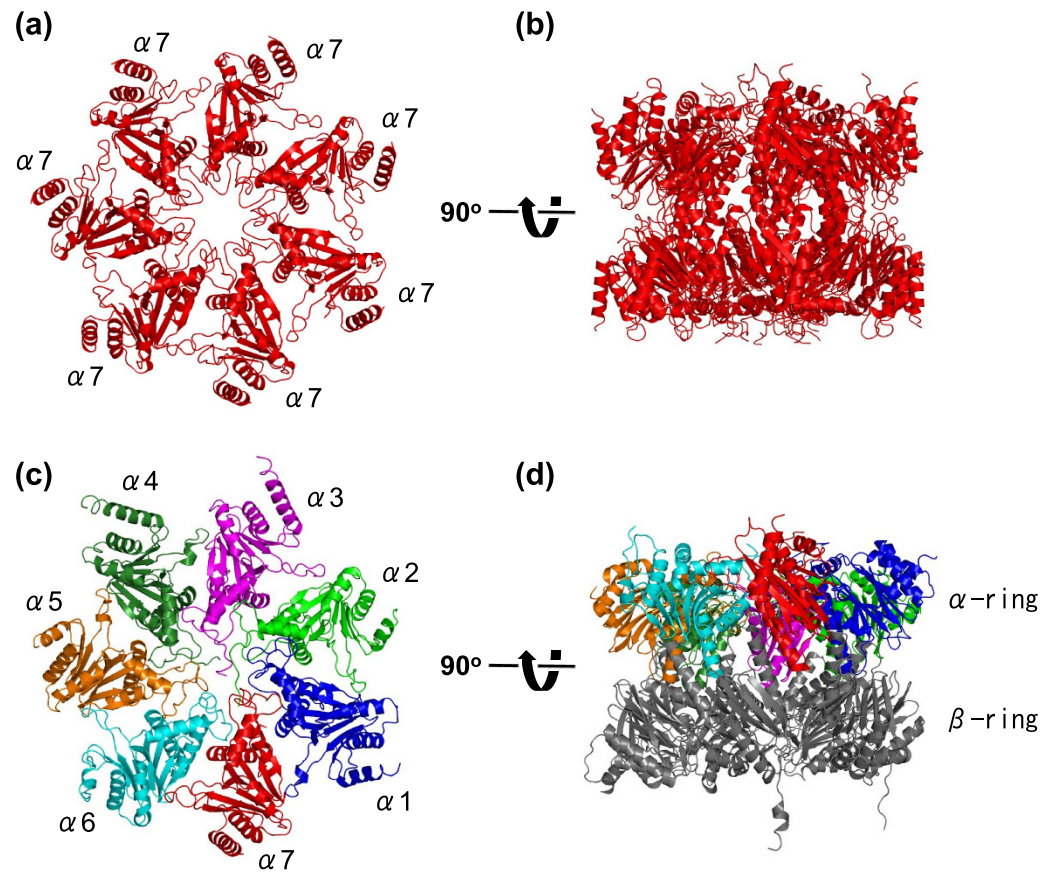


Figure 1. Crystal structure of the human $\alpha 7$ homo-tetradecamer. Ribbon models of the single and double $\alpha 7$ rings derived from the human $\alpha 7$ tetradecamer are shown in (a,b), respectively. Ribbon models of the $\alpha 1$ –7 ring and the $\alpha 1$ –7– $\beta 1$ –7 ring (half-proteasome) derived from the human 20S proteasome (PDB code 4R3O) are shown in (c,d), respectively. The left and right structures are related by a rotation of 90° around a horizontal axis. The α subunits are colored as follows: $\alpha 1$ (blue), $\alpha 2$ (green), $\alpha 3$ (magenta), $\alpha 4$ (forest green), $\alpha 5$ (orange), $\alpha 6$ (cyan), and $\alpha 7$ (red).

is lower than that in the MS method. In addition, recent sophisticated SV-AUC analyses have provided us with information regarding the structures of proteins and their complexes in solution, based on comparisons of experimentally estimated hydrodynamic parameters, e.g., sedimentation coefficient and diffusion constant, with those computed from their three-dimensional structure models¹².

Here we determine a crystal structure of the human $\alpha 7$ homo-tetradecamer and apply the complimentary MS and SV-AUC methods to investigate the oligomeric states of the proteasome α subunits, focusing on $\alpha 7$ and $\alpha 6$, its neighbor in the correctly arranged α -ring.

Results & Discussion

Structure determination of the $\alpha 7$ homo-tetradecamer. First, we determined the crystal structure of the human $\alpha 7$ tetradecamer at 3.75-Å resolution. The $\alpha 7$ tetradecamer exhibited an hourglass double-ring shape (Fig. 1a,b), which is consistent with the previously reported negative staining electron micrographs⁹ and small-angle neutron scattering (SANS) data¹⁰. The two α rings interact with each other mainly through two α helices that are involved in β -subunit interaction in the 20S proteasome^{5,13}. The conformations of the individual protomers and their quaternary arrangement in each ring of the human $\alpha 7$ tetradecamer are essentially identical with those observed in the homo-heptameric α -ring in archaeal proteasomes¹⁴ and the hetero-heptameric α -ring in mammalian proteasomes (Fig. 1c,d)^{5,13}.

Oligomeric states of proteasome $\alpha 7$ and $\alpha 6$ subunits. To characterize the oligomeric state of the $\alpha 7$ subunits in solution, we performed MS and SV-AUC analyses. The SV-AUC data showed that the $\alpha 7$ subunit exclusively exists as a single species with a sedimentation coefficient of 14.2 S (Fig. 2a), which is in excellent agreement with that estimated from the crystal structure (14.4 S), confirming the double-ring structure of this complex in solution. The mass spectrum of $\alpha 7$ under non-denaturing conditions exhibited ion series indicating

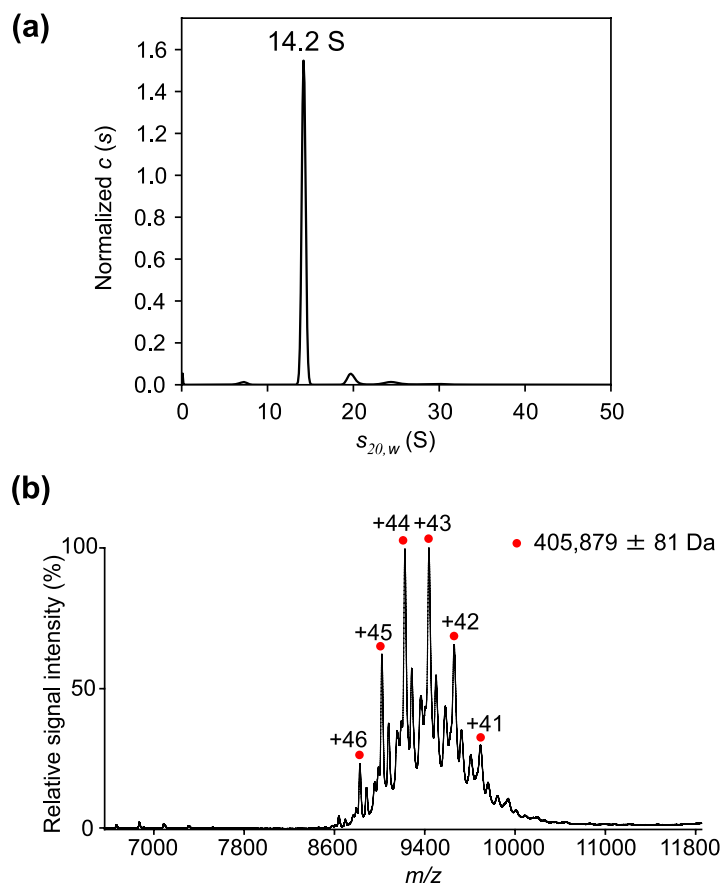


Figure 2. Characterization of the oligomeric state of the $\alpha 7$ subunit. (a) Distribution of $\alpha 7$ sedimentation coefficients derived from SV-AUC experiments. The 14.2 S peak corresponds to the $\alpha 7$ homo-tetradecamer. (b) Mass spectrum of $\alpha 7$ under non-denaturing conditions. Red circles show the ion series of the $\alpha 7$ homo-tetradecamer.

a complex with a molecular mass of $405,879 \pm 81$ Da (Fig. 2b). This confirms the homo-tetradecameric structure of this subunit (with a calculated mass of 28,284 Da, based on its amino acid sequence). Therefore, these results are consistent with the present crystal structure and the previously reported electron microscopy and solution scattering observations^{9,10}.

Furthermore, we examined the oligomeric state of the human proteasome $\alpha 6$ subunit, which makes direct contact with the $\alpha 7$ subunit in the proteasomal hetero-heptameric α -ring. The SV-AUC analysis showed that a majority of $\alpha 6$ exists as a monomer (2.6 S peak), while indicating that this subunit has a tendency to aggregate (Fig. 3a). The mass spectrum of $\alpha 6$ under non-denaturing conditions exhibited one major and one minor ion series, corresponding to the molecular masses of the monomer ($29,486 \pm 0$ Da) and dimer ($59,003 \pm 11$ Da), respectively (Fig. 3b).

To address the structural basis of the distinct oligomeric properties between $\alpha 6$ and $\alpha 7$, we made a hypothetical model of two $\alpha 6$ subunits brought into juxtaposition based on the homo-tetradecameric structure of $\alpha 7$ (Supplementary Fig. S1). Although a detailed comparison of the inter-subunit interaction modes was difficult because of the low resolution of the present crystal structure, the model clearly shows that $\alpha 6$ makes steric hindrances at the inter-subunit interface, thereby explaining why $\alpha 6$ is not able to form the homo-heptameric ring as $\alpha 7$ does.

Disassembly of the $\alpha 7$ double ring upon the addition of $\alpha 6$. Further, we attempted to characterize the oligomeric states of a mixture of $\alpha 7$ and $\alpha 6$ using SV-AUC and MS. The SV-AUC data indicated that the $\alpha 7$ homo-tetradecamer was less populated in the presence of $\alpha 6$, with the appearance of a smaller complex with a sedimentation coefficient of 10.2 S (Fig. 4a). In the MS analysis, the ion peak intensities of the $\alpha 7$ homo-tetradecamer were attenuated on titration with $\alpha 6$, with concomitant appearance of a new peak series (Fig. 4b). The molecular mass determined for this complex was $227,843 \pm 87$ Da, which corresponds to a 7:1 complex of $\alpha 7$ and $\alpha 6$ (with a calculated mass of 227,394 Da). All these data indicate that $\alpha 6$ interacts with $\alpha 7$, disassembling one mole of the tetradecameric double-ring of $\alpha 7$ and thereby give rise to two moles of the 1:7 hetero-octameric $\alpha 6$ - $\alpha 7$ complex. The mass spectrometric data showed that the $\alpha 7$ homo-tetradecamer was residual even in the presence of excess amount of $\alpha 6$, indicating that $\alpha 7$ was under equilibrium between the homo-tetradecameric state and the hetero-octameric form with $\alpha 6$ under the experimental condition. The mass spectra acquired at 60 min (upper)

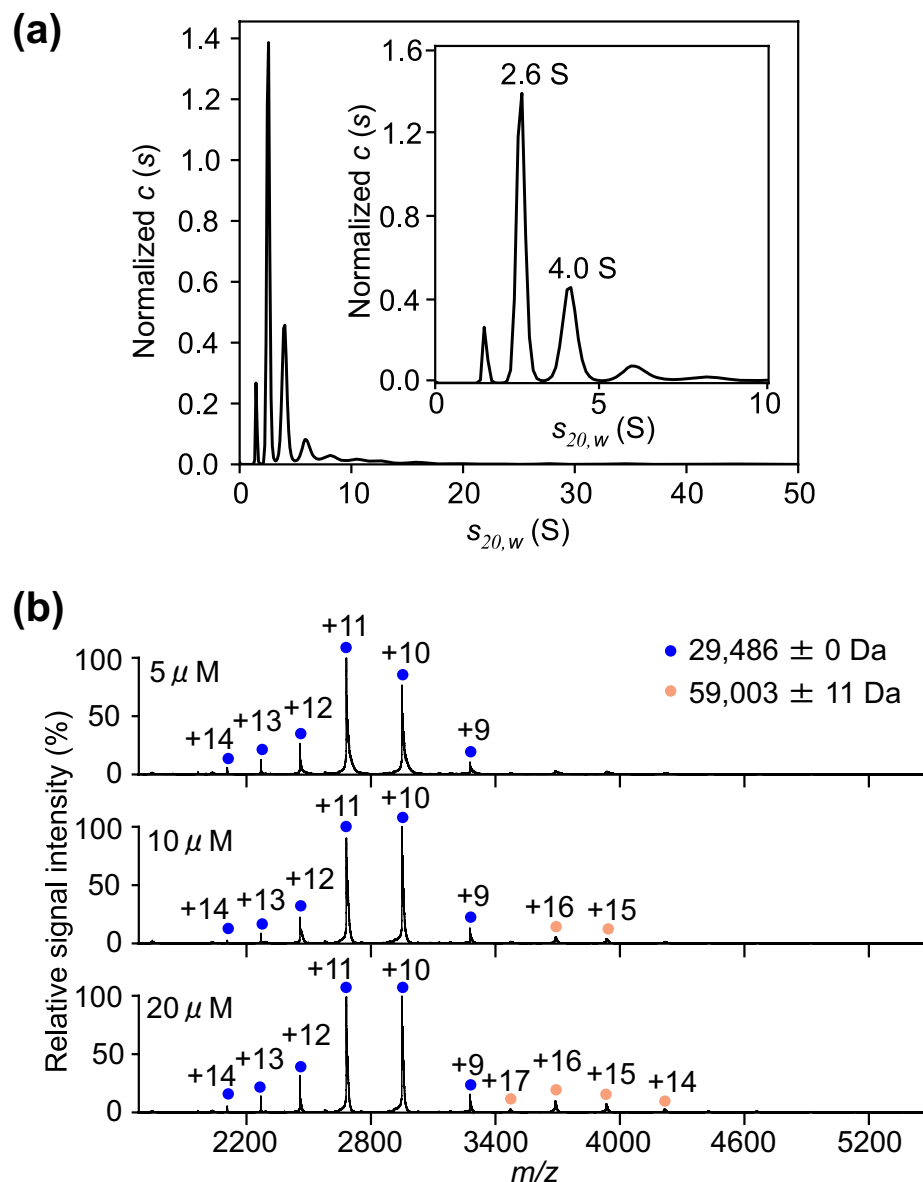


Figure 3. Characterization of the oligomeric state of the $\alpha 6$ subunit. (a) Distribution of $\alpha 6$ sedimentation coefficients derived from SV-AUC experiments. Inset shows the enlarged view with s -ranging from 0–10 displaying the peaks corresponding to monomer (2.6 S) and dimer (4.0 S) of $\alpha 6$. (b) Mass spectra of $\alpha 6$ at 5, 10, and 20 μ M under non-denaturing conditions. Blue and orange circles show the ion series of the $\alpha 6$ monomer and dimer, respectively.

and 115 min (lower) after mixing of $\alpha 6$ and $\alpha 7$ were virtually identical in terms of the population of the $\alpha 7$ homo-tetradecamer and the $\alpha 6$ - $\alpha 7$ hetero-octamer, implying that the system reached equilibrium within 60 min (Supplementary Fig. S2). The sedimentation coefficient of a single homo-heptameric $\alpha 7$ ring was calculated to be 8.9 S from the present crystal structure, suggesting that the 10.2 S hetero-octamer had a ring-shaped structure, although the position of $\alpha 6$ was uncertain.

Two alternative models for the disassembly of homo-heptameric $\alpha 7$ could be hypothesized. In one model, $\alpha 7$ exists in equilibrium between the double- and single-ring forms and $\alpha 6$ traps and stabilizes the single-ring species. However, our previous SANS data indicated that no detectable ring exchange occurred for 14 h after mixing deuterated and non-deuterated $\alpha 7$ homo-tetradecamers, indicating that the two heptameric rings are tightly associated with each other in the absence of the $\alpha 6$ subunit¹⁵. The other model is that $\alpha 6$ binds the $\alpha 7$ homo-tetradecamer and induces some type of allosteric conformational change at the ring-ring interface, resulting in the disassembly of the double-ring structure. Considering the stability of the $\alpha 7$ double-ring form in the absence of $\alpha 6$, the latter model is more plausible, although an $\alpha 6$ -bound homo-tetradecameric species of $\alpha 7$ could be detected in neither the SV-AUC profiles nor the mass spectra. Further kinetic and structural studies are necessary to identify the disassembly mechanism and quaternary structure of the $\alpha 6$ - $\alpha 7$ hetero-octamer.

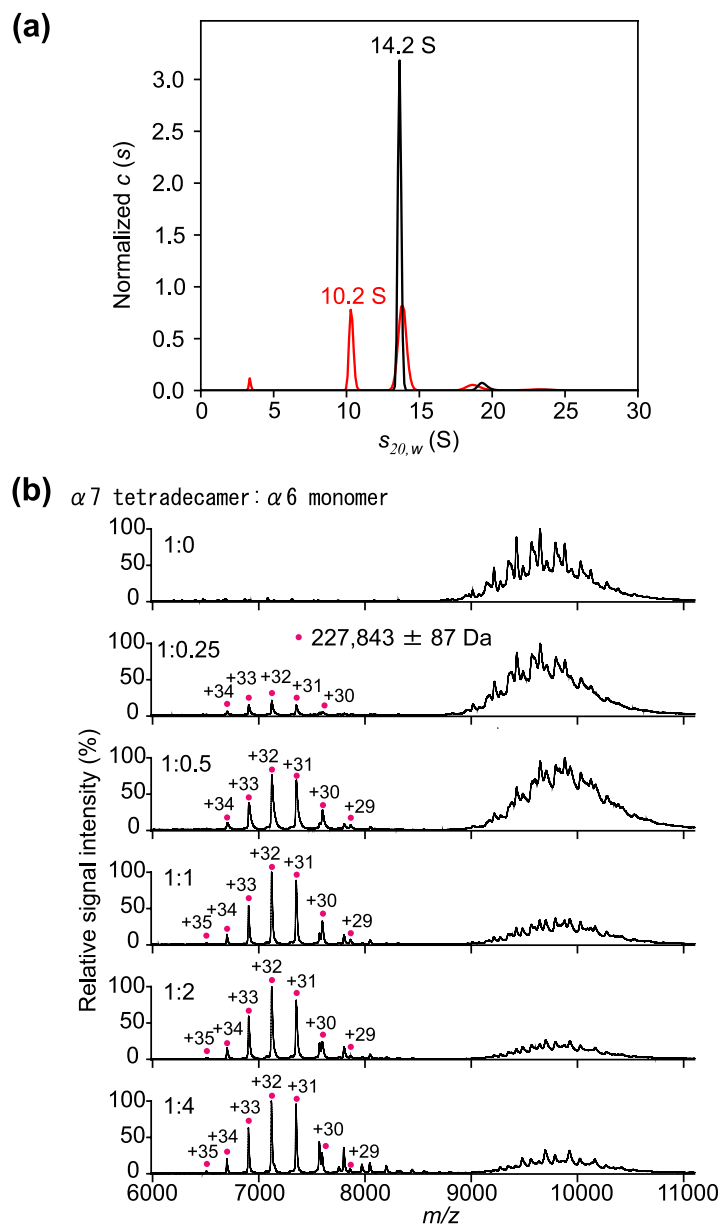


Figure 4. Characterization of the complex of $\alpha 7$ and $\alpha 6$ subunits. (a) Distribution of sedimentation coefficients of mixtures of $\alpha 7$ and $\alpha 6$ at 1:0 (black line) and 1:4 (red line) molar ratios ($\alpha 7$ tetradecamer to $\alpha 6$ monomer) derived from SV-AUC experiments. The 10.2 S and 14.2 S peaks correspond to the 1:7 hetero-octameric complexes of $\alpha 6$ and $\alpha 7$ and the $\alpha 7$ homo-tetradecamer, respectively. (b) Mass spectra of mixtures of $\alpha 7$ and $\alpha 6$ at 1:0, 1:0.25, 1:0.5, 1:1, 1:2, and 1:4 molar ratios ($\alpha 7$ tetradecamer to $\alpha 6$ monomer). Magenta circles show the ion series of the 1:7 hetero-octamer complexes of $\alpha 6$ and $\alpha 7$.

In summary, the present study demonstrates that the proteasome $\alpha 6$ subunit acts as a breaker of the $\alpha 7$ double-ring structure. Our findings suggest that proteasome formation involves disassembly processes of non-native oligomeric forms of proteasome subunits as assembly intermediates. The proteasome assembly pathway is a potential target for anticancer drug development^{16–18}. Therefore, our findings will provide new clues for drug discovery targeting the assembly/disassembly intermediates generated during proteasome formation.

Methods

Protein expression and purification. Human proteasome $\alpha 6$ short isoform and $\alpha 7$ subunits were expressed using *Escherichia coli* strain BL21-CodonPlus and purified as described previously^{10,15}. For the preparation of recombinant proteins, the cells were grown in Luria-Bertani medium. After sonication and centrifugation, cell lysates were subjected to anion-exchange chromatography (DEAE Sepharose Fast Flow, GE Healthcare). The proteins were further purified using an anion-exchange HPLC column (RESOURCE Q, GE Healthcare) and then with a gel-filtration HPLC column (HiLoad 26/60 Superdex 200 pg, GE Healthcare).

Crystallization, X-ray data collection, and structure determination. Native and selenomethione (SeMet)-substituted human $\alpha 7$ (10 mg/mL) was dissolved in 50 mM Tris-HCl (pH 7.4) and 150 mM NaCl. Crystals were grown in a buffer containing 24% PEG400, 100 mM Tris-HCl (pH 7.5), and 0.2 M magnesium chloride. These mixtures were incubated at 20 °C for approximately 1 week. The crystals were cryoprotected with the reservoir solution and flash-cooled in liquid nitrogen. The native and SeMet-substituted crystals belonged to space group $P4_32_12$, with one $\alpha 7$ tetradecamer per asymmetric unit. They diffracted at resolutions up to 3.75- and 4.20-Å resolution, respectively. Diffraction data were scaled and integrated using HKL2000¹⁹.

The 3.75-Å resolution crystal structure of the $\alpha 7$ tetradecamer was solved by the molecular replacement method using the program MOLREP²⁰ with a single α -ring of archaeal proteasome (Protein Data Bank code 1J2P)¹⁴ as the search model. Subsequently, fourteen bovine $\alpha 7$ subunit copies (PDB code 1IRU)⁵ were superimposed and then replaced with the archaeal α subunits. Model fitting to the electron density maps was performed using COOT²¹, in conjunction with the SeMet anomalous data. REFMAC5²² was used for the crystal structure refinement, and the stereochemical quality of the final model was validated using PROCHECK²³. The crystal parameters and refinement statistics are summarized in Supplementary Table S1. The molecular graphics were prepared using PyMOL (<http://www.pymol.org/>).

Sedimentation velocity analytical ultracentrifugation. Sedimentation analytical ultracentrifugation experiments were performed in 150 mM potassium phosphate (pH 7.4), using a ProteomeLab XL-I Analytical Ultracentrifuge equipped with four-hole An60 Ti rotor (Beckman Coulter). Solutions loaded in epon or aluminum centerpieces (Beckman Coulter) were run at 25,000 rpm for $\alpha 7$ and $\alpha 7 + \alpha 6$, and at 55,000 rpm for $\alpha 6$. Data were collected using an absorbance optical system at wavelengths where absorbance values were between 0.8 and 1.2. Data were analyzed using the continuous $c(s)$ distribution model in the program SEDFIT (version 14.4d). The partial specific volume of $\alpha 6$ and $\alpha 7$, buffer viscosity, and buffer density, calculated using the program SEDNTERP 1.09, were 0.73035 cm³/g, 0.71588 cm³/g, 1.013 cP, and 1.0009 g/mL, respectively. Hydrodynamic parameters were calculated from the crystallographic data with a program SOMO (SOLUTION MODeller) equipped with the UltraScan 3¹².

Mass spectrometry under non-denaturing conditions. The purified $\alpha 7$ and $\alpha 6$ proteins (420 μ M and 510 μ M monomer, respectively) were buffer-exchanged into 10 mM ammonium acetate, pH 6.8, and 150 mM ammonium acetate, pH 7.5, respectively, by passing the proteins through a Bio-Spin 6 column (Bio-Rad). The buffer-exchanged $\alpha 7$ (28 μ M monomer) and $\alpha 6$ (5, 10, and 20 μ M monomer) proteins were immediately analyzed by nanoflow electrospray ionization MS using gold-coated glass capillaries made in house (approximately 2–5 μ L sample loaded per analysis). Buffer-exchanged $\alpha 7$ (2 μ M tetradecamer) and $\alpha 6$ (0.5, 1, 2, 4, and 8 μ M monomer) at pH 7.5 were mixed, incubated at 20 °C for 1 h, and analyzed by nanoflow electrospray ionization MS. Spectra were recorded on a SYNAPT G2-Si HDMS mass spectrometer (Waters, Manchester, UK) in positive ionization mode at 1.33 kV with a 150 V sampling cone voltage and source offset voltage, 0 V trap and transfer collision energy, and 5 mL/min trap gas flow. The spectra were calibrated using 1 mg/mL cesium iodide and analyzed using Mass Lynx software (Waters).

References

- Pickart, C. M. Ubiquitin enters the new millennium. *Mol Cell* **8**, 499–504 (2001).
- Glickman, M. H. & Ciechanover, A. The ubiquitin-proteasome proteolytic pathway: destruction for the sake of construction. *Physiol Rev* **82**, 373–428 (2002).
- Baumeister, W., Walz, J., Zühl, F. & Seemüller, E. The proteasome: paradigm of a self-compartmentalizing protease. *Cell* **92**, 367–80 (1998).
- Groll, M. *et al.* Structure of 20S proteasome from yeast at 2.4 Å resolution. *Nature* **386**, 463–71 (1997).
- Unno, M. *et al.* The structure of the mammalian 20S proteasome at 2.75 Å resolution. *Structure* **10**, 609–18 (2002).
- Takagi, K. *et al.* Pba3-Pba4 heterodimer acts as a molecular matchmaker in proteasome α -ring formation. *Biochem Biophys Res Commun* **450**, 1110–4 (2014).
- Tomko, R. J. & Hochstrasser, M. Molecular architecture and assembly of the eukaryotic proteasome. *Annu Rev Biochem* **82**, 415–45 (2013).
- Hirano, Y. *et al.* Dissecting β -ring assembly pathway of the mammalian 20S proteasome. *EMBO J* **27**, 2204–13 (2008).
- Gerards, W. L. *et al.* The human α -type proteasomal subunit HsC8 forms a double ringlike structure, but does not assemble into proteasome-like particles with the β -type subunits HsDelta or HsBPROS26. *J Biol Chem* **272**, 10080–6 (1997).
- Sugiyama, M. *et al.* SANS simulation of aggregated protein in aqueous solution. *Nucl Instr Meth Phys Rev A* **600**, 272–274 (2009).
- Noda, M. *et al.* Assembly states of the nucleosome assembly protein 1 (NAP-1) revealed by sedimentation velocity and non-denaturing MS. *Biochem J* **436**, 101–12 (2011).
- Rocco, M. & Byron, O. Computing translational diffusion and sedimentation coefficients: an evaluation of experimental data and programs. *Eur Biophys J* **44**, 417–31 (2015).
- Harshbarger, W., Miller, C., Diedrich, C. & Sacchettini, J. Crystal structure of the human 20S proteasome in complex with carfilzomib. *Structure* **23**, 418–24 (2015).
- Groll, M., Brandstetter, H., Bartunik, H., Bourenkow, G. & Huber, R. Investigations on the maturation and regulation of archaeobacterial proteasomes. *J Mol Biol* **327**, 75–83 (2003).
- Sugiyama, M. *et al.* Kinetic asymmetry of subunit exchange of homooligomeric protein as revealed by deuteration-assisted small-angle neutron scattering. *Biophys J* **101**, 2037–2042 (2011).
- Besche, H. C., Peth, A. & Goldberg, A. L. Getting to first base in proteasome assembly. *Cell* **138**, 25–8 (2009).
- Gallastegui, N. & Groll, M. The 26S proteasome: assembly and function of a destructive machine. *Trends Biochem Sci* **35**, 634–42 (2010).
- Doi, T. *et al.* Total synthesis and characterization of thielocin B1 as a protein-protein interaction inhibitor of PAC3 homodimer. *Chem Sci* **5**, 1860–1868 (2014).
- Otwinowski, Z. & Minor, W. Processing of X-ray diffraction data collected in oscillation mode. *Methods Enzymol* **276**, 307–326 (1997).
- Vagin, A. & Teplyakov, A. MOLREP: An automated program for molecular replacement. *J Appl Crystallogr* **30**, 1022–25 (1997).

21. Emsley, P., Lohkamp, B., Scott, W. G. & Cowtan, K. Features and development of Coot. *Acta Crystallogr D Biol Crystallogr* **66**, 486–501 (2010).
22. Murshudov, G. N., Vagin, A. A. & Dodson, E. J. Refinement of macromolecular structures by the maximum-likelihood method. *Acta Crystallogr D Biol Crystallogr* **53**, 240–55 (1997).
23. Laskowski, R. A., MacArthur, M. W., Moss, D. S. & Thornton, J. M. PROCHECK: a program to check the stereochemical quality of protein structures. *J Appl Cryst* **26**, 283–291 (1993).

Acknowledgements

We thank Dr. Keiji Tanaka (Tokyo Metropolitan Institute of Medical Science) for providing the human proteasome $\alpha 6$ and $\alpha 7$ subunit expression systems and Drs. Tsunehiro Mizushima (University of Hyogo, Japan) and Masato Kawasaki (KEK, Tsukuba, Japan) for their help with X-ray data collection at the synchrotron facilities. Diffraction datasets were collected at NSRRC using beamline 13B1 and SPring-8 BL44XU (Japan). We thank Drs. Eiji Kurimoto and Kenta Okamoto (Nagoya City University, Japan) for their contributions at the early stage of this study and Dr. Rintaro Inoue (Kyoto University, Japan) for useful discussion. Furthermore, we thank Kiyomi Senda, and Kumiko Hattori (Nagoya City University, Japan) for their help during the preparation of the recombinant proteins. This work was supported by grants (25102001, 25102008, and 15H02491 to K.K. and 25121722 and 26102530 to S.U.) from the Ministry of Education, Culture, Sports, Science and Technology (MEXT) of Japan, by the Okazaki ORION project, and by the Joint Studies Program (2014–2015) in the Okazaki BIO-NEXT project of the Okazaki Institute for Integrative Bioscience.

Author Contributions

K.K. and S.U. conceived and designed the experiments; K.I. and H.Y. prepared the samples; R.T., S.S. and T.S. performed the crystallographic analysis; K.I., M.N. and S.U. performed the mass analysis; M.N. and S.U. performed the ultracentrifugation analysis; all authors wrote and reviewed the manuscript.

Additional Information

Supplementary information accompanies this paper at <http://www.nature.com/srep>

Accession codes: The coordinate and structural factor of the crystal structure of human $\alpha 7$ homo-tetradecamer has been deposited in the Protein Data Bank under accession number 5DSV.

Competing financial interests: The authors declare no competing financial interests.

How to cite this article: Ishii, K. *et al.* Disassembly of the self-assembled, double-ring structure of proteasome $\alpha 7$ homo-tetradecamer by $\alpha 6$. *Sci. Rep.* **5**, 18167; doi: 10.1038/srep18167 (2015).



This work is licensed under a Creative Commons Attribution 4.0 International License. The images or other third party material in this article are included in the article's Creative Commons license, unless indicated otherwise in the credit line; if the material is not included under the Creative Commons license, users will need to obtain permission from the license holder to reproduce the material. To view a copy of this license, visit <http://creativecommons.org/licenses/by/4.0/>